



VICTORIA UNIVERSITY
MELBOURNE AUSTRALIA

MUC1 expressing tumor growth was retarded after human mucin 1 (MUC1) plasmid DNA immunization

This is the Published version of the following publication

Son, Hye-Youn, Jeong, Hwan-Kyu, Apostolopoulos, Vasso and Kim, Chul-Woo (2022) MUC1 expressing tumor growth was retarded after human mucin 1 (MUC1) plasmid DNA immunization. *International Journal of Immunopathology and Pharmacology*, 36. ISSN 0394-6320

The publisher's official version can be found at
<https://journals.sagepub.com/doi/10.1177/03946320221112358>
Note that access to this version may require subscription.

Downloaded from VU Research Repository <https://vuir.vu.edu.au/46754/>

MUC1 expressing tumor growth was retarded after human mucin I (MUC1) plasmid DNA immunization

International Journal of
Immunopathology and Pharmacology
Volume 36: 1–15
© The Author(s) 2022
Article reuse guidelines:
sagepub.com/journals-permissions
DOI: 10.1177/03946320221112358
journals.sagepub.com/home/iji
SAGE

Hye-Youn Son^{1,†} , Hwan-Kyu Jeong^{2,†} , Vasso Apostolopoulos³  and Chul-Woo Kim⁴

Abstract

Introduction: Naked DNA is one of the attractive tools for vaccination studies. We studied naked DNA vaccination against the human tumor antigen, mucin, which is encoded by the *MUC1* gene.

Methods: We constructed the pcDNA3.0-MUC1 (pcDNA-MUC1) plasmid expressing an underglycosylated MUC1 protein. BALB/c mice were immunized intradermally thrice at 2-weeks intervals with pcDNA-MUC1. Two weeks after the last immunization, tumor challenge experiments were performed using either the CT26 or TA3HA tumor cell lines, both of which transduce human MUC1.

Results: Immune cell population monitoring from pcDNA-MUC1-immunized animals indicated that immune cell activation was induced by MUC1-specific immunization. Using intracellular fluorescence activated cell sorting and enzyme-linked immunosorbent spot assay, we reported that interferon- γ secreting CD8⁺ T cells were mainly involved in MUC1-specific immunization. In all mice immunized with *MUC1* DNA, tumor growth inhibition was observed, whereas control mice developed tumors ($p < 0.001$).

Conclusion: Our results suggest that intradermal immunization with *MUC1* DNA induces MUC1-specific CD8⁺ T cell infiltration into tumors, elicits tumor-specific Th1-type immune response, and inhibits tumor growth.

Keywords

MUC1, DNA vaccines, CD8 T cells, Tumor retardation

Date received: 23 February 2022; accepted: 16 June 2022

Introduction

To develop effective immunotherapy, we often include a tumor antigen in the construction of vaccines against cancer. The human *MUC1* gene contains the sequence of a large transmembrane polypeptide (>400 kDa) consisting of a uneven number of 20 amino acids tandem repeats.¹ MUC1 is expressed on a variety of epithelial-derived cells and is heavily glycosylated in the benign state; its distribution is restricted to the apical surface of the ductal cells.² In contrast, in the malignant state, the expression of

¹Department of Breast and Endocrine Surgery, Center for Medical Innovation, Seoul National University Hospital, Seoul, South Korea
²School of Biosystems and Biomedical Sciences, Korea University, Seoul, South Korea

³Institute for Health and Sport, Victoria University, Melbourne, Vic, Australia

⁴BIOINFRA Life Science Inc., Seoul, South Korea

[†]These authors contributed equally to this work.

Corresponding author:

Chul-Woo Kim, BIOINFRA Life Science Inc., Daehak-ro 49, Jongno-gu, Seoul 03127, South Korea.

E-mail: chulwoo.kim@bioinfra.co.kr



Creative Commons Non Commercial CC BY-NC: This article is distributed under the terms of the Creative Commons Attribution-NonCommercial 4.0 License (<https://creativecommons.org/licenses/by-nc/4.0/>) which permits non-commercial use, reproduction and distribution of the work without further permission provided the original work is attributed as specified on the SAGE and Open Access pages (<https://us.sagepub.com/en-us/nam/open-access-at-sage>).

underglycosylated MUC1 is increased which is distributed along the entire surface of cells.³ Underglycosylation of MUC1 lead to unmasking novel epitopes on the protein in breast malignancies which is unique to the malignant state.⁴ In such malignant form, MUC1 has been revealed to be immunogenic with each tandem repeat containing epitopes.⁵ As MUC1 antibodies have been seen in breast cancer patients albeit at a low rate, it has been suggested that underglycosylated MUC1 may be capable of stimulating a potent immune response.⁶ In this manner, it is possible to target MUC1 for vaccine immunotherapy, and several attempts have been made by using MUC1 as a cancer vaccine.⁷ Most of them have focused on the use of a synthetic peptide including several tandem repeats, with some of them conjugated to a carrier protein.^{8–10} These MUC1 vaccines have been revealed to stimulate a modest humoral response. However, it is challenging to assure that the immune response provoked is targeted specifically for the tumor cells without adverse effects on the host.^{11–13}

DNA vaccines are proposed to be more appropriate for clinical use than other methods, such as vaccines with peptides or autologous cancer cells, or the adoptive transfer of cytotoxic T lymphocytes for several reasons: (a) when the DNA vector is ready, DNA vaccines are affordable and simple to use; (b) autologous immune cells, cancer cells, or adjuvants are not needed; (c) high levels of antigen expression can be retained; and (d) DNA vaccination does not require facilities and techniques for cell culture. Thus, it is reasonable to present that DNA vaccination targeting tumor antigens has significant potential for anticancer immunotherapy.¹⁴

Vaccination with tumor antigens-encoding DNA has been suitable for maintaining high levels of tumor antigen expression at the vaccination site and eliciting immune response, especially cellular immunity specific to the antigens encoded by the DNA.^{15,16} Attempts at using viral vectors have achieved limited success, except those that involve DNA insertion into the host genome.¹⁷ Finn et al. reported that the MUC1 protein was expressed by host cells infected with MUC1 viral vectors; consequently, they expressed heterogeneous glycosylated target proteins, proposing a variable glycosylation pattern or instability in the recombinant protein expression. Thus, the viral vectors induced relatively low potency of tumor immunity as stimulation of multiple T cell epitopes occurred simultaneously.¹⁸

This study reported the use of naked *MUC1* plasmid DNA containing 42 tandem repeats as a tumor vaccine. It delivers the underglycosylated form of the corresponding protein showing homogenous patterns of glycosylation. After three vaccinations, we evaluated the growth inhibition of similar *MUC1* gene-transduced tumor cells in a xenograft model. In addition, this study proves for the first time that using immunohistochemistry to induce CD8⁺ T

cell infiltration into the tumor mass is important for tumor retardation.

Materials and methods

This mice-based study was performed based on analysis of a database of cancer patients which showed the importance of MUC1 during cancer progression. After immunizing MUC1-transduced cells into mice, we examined the effectiveness of the MUC1 DNA vaccine through several experiments such as western blotting and fluorescence activated cell sorting (FACS).

cBioPortal database analysis

Cancer genomics analysis was performed by querying the online cBioPortal for Cancer Genomics (<http://www.cbioportal.org/>; date last accessed, 2 January 2022). The cBioPortal for Cancer Genomics is associated with the Memorial Sloan Kettering Cancer Center and provides comprehensive analyses of complex tumor genomics and clinical profiles from research on 105 cancer types in The Cancer Genome Atlas (TCGA). cBioPortal was used to identify which type of cancer would be more effective in DNA vaccine and guide further study. TCGA PanCancer Atlas Studies were firstly used to examine which type of cancer is related to *MUC1* gene alteration. Subsequently, a more detailed search was performed based on 24 studies, including 14 breast cancer studies and 10 colon cancer studies.^{19–47} The data used included the following: Breast Cancer (MSK, Cancer Cell 2018)²¹; Breast Cancer (MSK, Nature Cancer 2020)²²; Breast Cancer Xenografts (British Columbia, Nature 2015)²³; Breast Invasive Carcinoma (Broad, Nature 2012)²⁴; MAPK on Resistance to Anti-HER2 Therapy for Breast Cancer (MSKCC, Nat Comm 2021)²⁵; Metastatic Breast Cancer (MSK, Cancer Discovery 2021); Breast Cancer (SMC 2018)²⁶; Breast Invasive Carcinoma (TCGA, Firehose Legacy); Breast Cancer (MSK, Clinical Cancer Res 2020)²⁷; Breast Cancer (MSKCC, NPJ Breast Cancer 2019)²⁸; Breast Invasive Carcinoma (British Columbia, Nature 2012)²⁹; Breast Cancer (METABRIC, Nature 2012 & Nat Commun 2016)^{30–32}; Breast Invasive Carcinoma (Sanger, Nature 2012)³³; The Metastatic Breast Cancer Project (Provisional, February 2020); Colon Adenocarcinoma (CaseCCC, PNAS 2015)³⁴; Colon Cancer (CPTAC-2 Prospective, Cell 2019)³⁵; Colorectal Adenocarcinoma (DFCI, Cell Reports 2016)³⁶; Colorectal Adenocarcinoma (Genentech, Nature 2012)³⁷; Colorectal Adenocarcinoma Triplets (MSKCC, Genome Biol 2014)³⁸; Colorectal Cancer (MSK, Gastroenterology 2020)³⁹; Disparities in metastatic colorectal cancer between Africans and Americans (MSK, 2020); Metastatic Colorectal Cancer (MSKCC, Cancer Cell 2018)⁴⁰; Rectal

Cancer (MSK, Nature Medicine 2019)⁴¹; and Colorectal Adenocarcinoma (TCGA, Nature 2012).⁴²

Prognoscan database analysis

Prognoscan (<http://www.prognoscan.org/>; date last accessed, 7 February 2022) is an online database for investigating underlying tumor indicators and therapeutic targets. It is a large collection of cancer microarray datasets that are collected from the public domain with clinical annotation and assesses the relationship between the expression of certain genes and prognosis using the minimum *p*-value approach. The Prognoscan database was searched to confirm the significance of *MUC1* alteration in patients with breast and colon cancers. This tool allowed the expression of *MUC1* to be divided into “high” or “low,” according to the median expression of the genes. Blue and red curves correspond to low and high *MUC1* expressions, respectively.⁴⁸

MUC1 constructs

Schematic diagrams of plasmids pcDNA3.0-*MUC1* (pcDNA-*MUC1*) and pLXIN-*MUC1* are illustrated in Figure 2(a) and (b), respectively. The human *MUC1* gene, with 42 tandem repeats (accession no. J05582), was cloned techniques into the *Bam*HI site of plasmid vector pcDNA3.0 (Invitrogen) through standard subcloning, and was designated pcDNA-*MUC1*. All restriction enzymes were obtained from New England Biolabs (Beverly, MA), and the reactions were performed according to the manufacturer’s guidelines. For the retroviral construct, the same procedure was performed, except that the retroviral vector pLXIN (Invitrogen) was used to clone the *MUC1* gene; the construct was designated pLXIN-*MUC1*. All DNA constructs were investigated by BamHI restriction mapping and sequencing to confirm the correct insert.

MUC1-transduced cells

Packaging cell line PA317 (CRL-9078) was transfected with the pLXIN-*MUC1* construct using lipofectamine (Life Technologies, CA) and grown in 10% fetal bovine serum (FBS)-supplemented Dulbecco’s Modified Eagle Medium (DMEM) containing G418. The most productive clones, as determined by reverse transcriptase polymerase chain reaction (RT-PCR), were selected and cultured to obtain the *MUC1*-containing virus particles. Target cell lines CT26 (murine colon carcinoma, H-2d, KCLB 8000) and TA3HA (murine mammary carcinoma, H-2d, CVCL_4321) were transduced with viral supernatants in the presence of 8 µg/ml polybrene. The quantity of G418 used was 1200 µg/ml for CT26 and TA3HA. After

being transferred to 10-mm dishes, each clone was cultured under G418-containing media supplemented with 10% FBS to establish stable cell lines expressing human *MUC1*, which were designated CT26-*MUC1* and TA3HA-*MUC1*.

MUC1 cell surface expression

Two hundred and ninety-three cells originating from Human kidney were transiently transfected with the pcDNA-*MUC1* using lipofectamine (Life Technologies, CA) and grown in 10% FBS-supplemented DMEM for 48 h. The cell surface expression of *MUC1* was determined on both established (CT26, TA3HA) and transient-transfected (293) *MUC1*-expressing cells. Moreover, 5×10^5 cells were incubated with anti-*MUC1* antibodies for 30 min at 4°C; isotype-matched antibodies were used as a negative control. Anti-*MUC1* monoclonal antibody for the non-glycosylated backbone was purchased from BIOMEDA (BIOMEDA, USA). After washing with 0.1% bovine serum albumin-phosphate-buffered saline (BSA-PBS), cells were incubated with anti-mouse fluorescence conjugates (BD Pharmingen, CA) for 30 min at 4°C. After washing with 0.1% BSA-PBS, cells were fixed with 2% paraformaldehyde-PBS.⁴⁵ Staining was analyzed using a Coulter EPICS XL Flow Cytometer (BD Coulter, FL).

Western blotting

Cell lysates were prepared from both established and transient-transfected *MUC1*-expressing cells using lysis buffer. Equal aliquots were resuspended with sodium dodecyl sulfate (SDS) sample buffer and boiled for 10 min. The supernatant was loaded on an 8% SDS gel, and the protein was separated by electrophoresis. Molecular mass was determined by calibration of the gels with protein standards. When electrophoresis was completed, the proteins were transferred to a nitrocellulose membrane (Bio-Rad Laboratories, CA), and non-specific sites were blocked with 5% non-fat powdered milk and 0.1% Tween 20 in Tris-buffered saline (TTBS). The presence of *MUC1* was determined by immunoblotting with anti-*MUC1* antibodies, similar to flow cytometry, and Erk1/2 with an anti-mouse Erk1/2 mouse antibody (Sigma, MO) was used to control protein integrity. After completion of the primary incubation overnight at 4°C, the membranes were washed with TTBS and incubated with goat anti-mouse peroxidase-labeled secondary antibody (Amersham Pharmacia Biotech, NJ) for 1 h at 25°C. The immunoblot was developed by the enhanced chemiluminescence method (Amersham Pharmacia Biotech, NJ) as directed by the manufacturer.

Immunization

Specific pathogen-free 6-week-old female BALB/c mice were obtained from SLC (Japan) and handled under specific pathogen-free conditions according to the guidelines issued by the Seoul National University Animal Research Committee. Mice were intradermally administered 100 µg of pcDNA-MUC1 suspended in 50 µL of endotoxin-free tris-ethylenediaminetetraacetic acid (TE; QIAGEN) into each thigh using a 30-G insulin syringe (Becton Dickinson, NJ) three times at 2-weeks intervals. Anesthesia was induced by injecting 0.3 mL of 1:1:9 solution of Rompun (Parke Davis, Germany), ketamine (Bayer, Germany), and saline (RKS) intraperitoneally.

In vivo MUC1 location

The skin near the injection site was taken from immunized mice and digested for 72 h at 56°C with 0.1 mg/mL proteinase K in 0.1 M Tris-acetate buffer, pH 7.5, 0.2% SDS, 5 mM ethylenediamine tetra acetic acid, and 200 mM sodium chloride. DNA was phenol-chloroform extracted, precipitated with 0.1 volume of isopropanol, and re-suspended in TE buffer (pH 8.0). The MUC1 DNA location was detected by PCR using the specific primers GGCTCCTCGGTGACTCTAGGATGC (forward) and CATGAATTCTGGGCTCAATTTTCTTGTC (reverse). To control DNA integrity, the mouse β-actin gene (codons 135–223) was amplified using the primers GGCTCCTCGGTGACTCTAGGATGC (forward) and CATGAATTCTGGGCTCAATTTTCT-TGTC (reverse). PCR conditions used were 34 cycles of 60 s at 94°C, 60 s at 55°C, and 60 s at 72°C.

In vivo MUC1 expression

The skin near the injection site was taken from immunized mice and lysed using a homogenizer. Total RNAs were extracted from lysates in the presence of RNase inhibitors according to the TRIzol reagent protocol (Molecular Research Center, OH). RNAs were dissolved in diethyl pyrocarbonate (Sigma-Aldrich, MO)-treated water. cDNA was generated from an mRNA template using a 15-mer poly-dT oligonucleotide (Invitrogen, CA) and superscript reverse transcriptase enzyme (GIBCO-BRL, CA) at 37°C for 1 h using the SuperScript Preamplification System protocol. MUC1 gene expression was detected by PCR using the same primers and protocols as described above.

Anti-MUC1 antibody

Serum from immunized mice was collected 5 days after the third injection and tested for MUC1 antibody levels by enzyme-linked immunosorbent assay (ELISA). Blood was

allowed to clot overnight at 4°C. The serum was then removed and stored frozen at –20°C until use. The ELISA test was performed as described elsewhere.⁴⁶ Briefly, 10 µg/mL peptide (CT1-30; PDTRPAPGSTAPPAHGVTSPDTRPAPGSTA) contained one repeat and 10 amino acids from the next repeat of the VNTR, 1 mg/mL MUC1 fusion protein was coated in the wells of a microtiter plate, nonspecific binding was blocked with 2% bovine serum albumin, and serial dilutions of serum were added for 2 h at 15–22°C. After washing, goat-anti mouse Igs (Sigma–Aldrich) were added and then re-washed, and rabbit anti-goat IgG conjugated with horseradish peroxidase (Amersham Bioscience, Sweden) was added. The reaction was developed using a chromogen substrate kit (3,3',5,5'-tetramethylbenzidine solution and hydrogen peroxide; Bio-Rad Life Sciences, CA). Absorbance was read at 450 nm versus the reference absorbance at 620 nm using a Multiskan EX/RC (Labsystems, Finland).

Fluorescence activated cell sorting (FACS)

Cells were washed with 0.1% BSA-PBS and stained with suitable antibodies (CD3, CD22, CD4, CD8, or CD40) in the dark and on ice for 30 min. Cells were centrifuged twice and washed with 0.1% BSA-PBS. Cells were detected using the FACSCanto system (BD, NJ).

Intracellular FACS

CD3 cell surface antigen staining was performed as described above, and cells were fixed in a 0.5 mL/tube Fixation Buffer (BioLegend, SD) in the dark for 20 min at room temperature and centrifuged at 350 ×g for 5 min. The supernatant was discarded. Fixed cells were re-suspended in Intracellular Staining Perm Wash Buffer (BioLegend, SD) and centrifuged at 350 ×g for 5–10 min. Fixed/permeabilized cells were re-suspended in residual Intracellular Staining Perm Wash Buffer, and 5 µL of fluorophore-conjugated antibody of interest (interferon [IFN]-γ or interleukin [IL]-4) was added for 20 min in the dark at room temperature. Moreover, 2 mL of Intracellular Staining Perm Wash Buffer was washed and centrifuged at 350 ×g for 5 min. Fixed and intracellularly labeled cells were re-suspended in 0.5 mL Cell Staining Buffer. Cells were centrifuged twice and washed with 0.1% BSA-PBS. The stained cells were detected using FACSCanto (BD, NJ).

Enzyme-linked immune absorbent spot (ELISpot) assay

The spleen, non-draining lymph nodes (LNs), and draining LNs were extracted from mice 10 days after the third

injection and tested for MUC1-specific cytokine-producing lymphocytes. The enzyme-linked immune absorbent spot (ELISpot) assay was performed, as described elsewhere.^{47,48} Briefly, to assess IFN- γ secretion, MultiScreen-IP plates (poly [vinylidene fluoride] membranes, Millipore) were coated overnight at 4°C with 50 μ L/well of anti-human IFN- γ or IL-4 capture antibody (Biosource, International, Camarillo CA) diluted at 2 μ g/mL in PBS. After overnight incubation at room temperature, coated plates were washed and blocked as described above. Effector cells (100 μ L/well) were added at specified concentrations followed by 5×10^4 target cells per well (100 μ L). After the effector and target cells were incubated at 37°C, the plates were washed with PBS + 0.05% Tween 20 and 50 μ L/well of biotinylated anti-human IFN- γ or IL-4 detecting antibody (PharMingen, San Jose, CA) diluted to 1.3 μ g/mL in PBS with 1% BSA, and 0.05% Tween 20 was added. Plates were incubated with detecting antibody for 2 h at room temperature and washed four times with PBS, and 50 μ L of streptavidin-alkaline phosphatase (Gibco BRL Life Technologies) diluted with 1:1500 in PBS with 1% BSA was added. After 1-h incubation at room temperature with streptavidin-alkaline phosphatase, the plates were washed and the spots were visualized and enumerated, as stated above.

Tumor challenge

Two weeks after the final *MUC1* DNA injection, mice were challenged subcutaneously with 5×10^4 or 5×10^5 CT26-MUC1 cells or 1×10^5 TA3HA cells suspended in 100 μ L of PBS. Tumors were measured twice a week, and tumor sizes (mm^3) were calculated using horizontal (mm) \times vertical (mm) \times depth (mm).

Statistical analyses

The Mann–Whitney U method was used in this study. Polynomial regression analysis of tumor size over time and within groups showed a p value < 0.001 .

Results

MUC1 is related to several types of cancers, including breast and colorectal cancers

We first searched for *MUC1* gene alteration counts to specify what type of cancer would be effective in *MUC1* DNA vaccine. From the TCGA PanCancer Atlas Studies, which include samples from 10,953 patients, *MUC1* was identified as being modified in different types of cancers, including hepatocellular carcinoma, endometrial carcinoma, and non-small cell lung cancer. Colon cancer also presented relatedness with *MUC1* alteration (blue box),

and invasive breast carcinoma seems to be the type highly related to *MUC1* alteration (red box; Figure 1(a)). We then selected samples from breast and colon cancers with detailed subtypes. By comparing 8125 samples of human breast cancer from 14 different studies and 3254 samples of human colon cancer from 10 different studies, breast invasive ductal carcinoma, colon adenocarcinoma, and colorectal adenocarcinoma primarily showed *MUC1* gene alteration. Breast invasive lobular carcinoma also showed close relevance with *MUC1* alteration following breast invasive ductal carcinoma. Both truncating and missense mutation types were observed in colon and colorectal adenocarcinomas. Truncating mutations were presented in one patient of each subtype, and missense mutations were mainly shown in 12 patients with colorectal adenocarcinoma. The plot chart comparing each of the breast cancer samples demonstrated that the missense mutant type was only observed in breast invasive ductal carcinoma. An amplification, a mutation that increases the copy number of a specific DNA segment (mostly in cancer cells), was observed in breast invasive ductal carcinoma, as shown in the red circle. Therefore, *MUC1* alterations, specifically missense and amplification mutations, are identified to be highly related to breast invasive ductal carcinoma (Figure 1(b)).

Additionally, the relationship between *MUC1* alteration and human breast and colon cancers was specified among groups of different races. Asians comprised a larger fraction of individuals in the *MUC1* unaltered group (21.55%) than in the *MUC1* altered group (8.26%), with a p value of 5.541×10^{-4} . The opposite tendency was observed in African Americans; they comprised 23.14% of the altered group, which is higher than their proportion in the unaltered group (14.06%) (Figure 1(c)).

Finally, the prognostic value of *MUC1* expression has been reported by the PrognoScan database. In the present study based on microarray data, increased expression of *MUC1* mRNA was significantly associated with decreased overall survival (OS), disease-free survival (DFS), and disease-specific survival (DSS) in breast cancer. The OS tendency was similar in the high and low groups in colon cancer. However, the DFS and DSS plots showed that the group with high *MUC1* expression had a lower survival rate (Figure 1(d)). Therefore, *MUC1* gene alteration appears to be related to several types of human cancers, including breast and colon cancers, and further experiments were conducted to examine the effectiveness of the *MUC1* DNA vaccine.

In vitro MUC1 expression

The presence of DNA inserts for *MUC1* cDNA (N- and C-termini and 42 tandem repeats) was confirmed from both

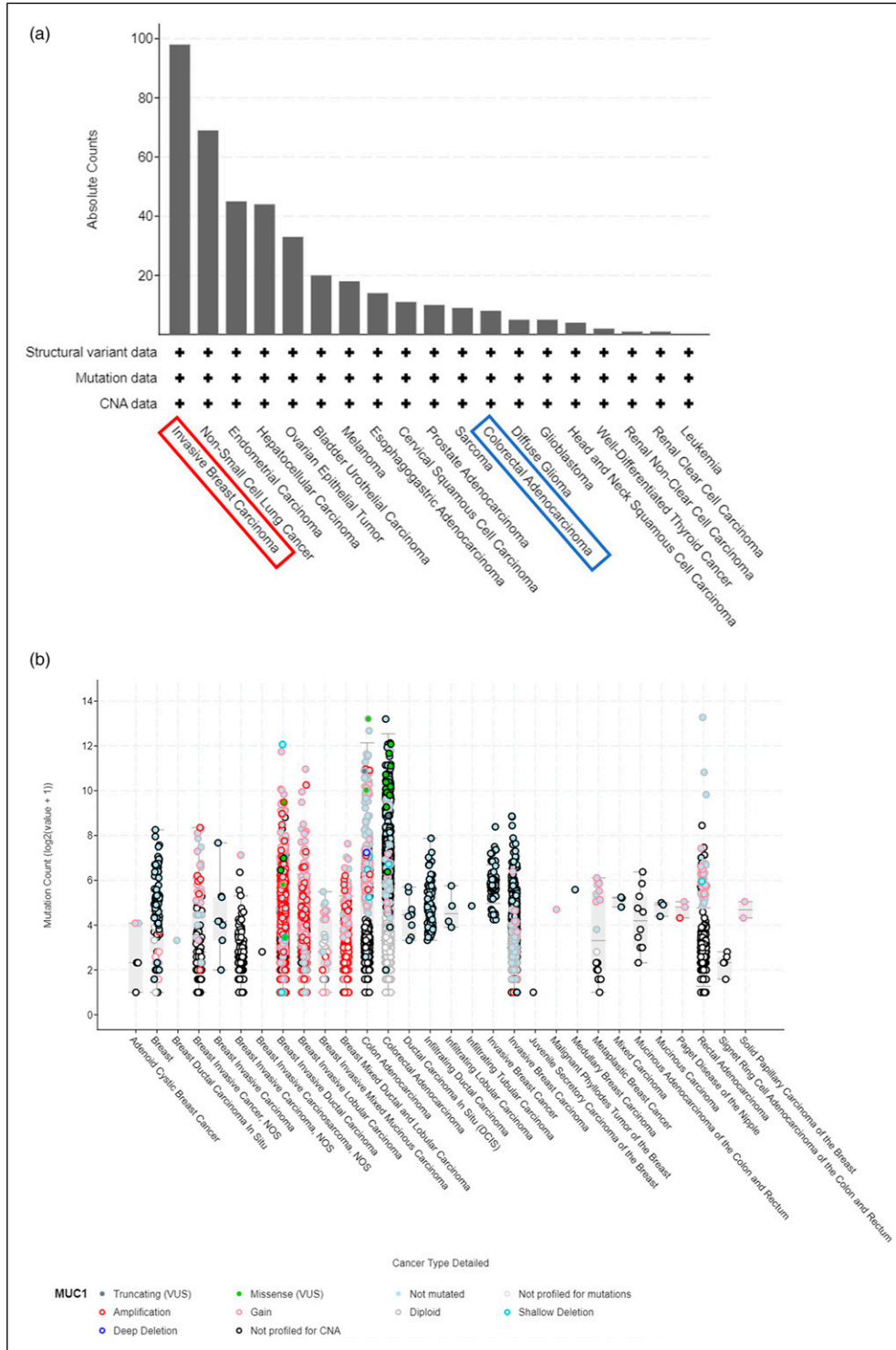


Figure 1. TCGA PanCancer Atlas Studies with minimal total count set as 200. (a) Samples from 10,953 patients from the TCGA PanCancer Atlas Studies were used. The data contain invasive breast carcinoma, non-small cell lung cancer, endometrial carcinoma, hepatocellular carcinoma, prostate carcinoma, and colorectal adenocarcinoma. (b) Log scale value of mutation count was classified into several subtypes. The circle indicates which type of mutation occurred in each sample (green for missense and red for amplification). (c) The number of samples was divided into groups of different races such as American Indian, Alaska native, Asian, African American, and White. (d) Prognostic significance of *MUC1* gene expression in patients with breast and colorectal cancer (OS, DFS, and DSS time in the PrognScan database). OS, overall survival; DFS, disease-free survival; DSS, disease-specific survival; HR, hazard ratio.

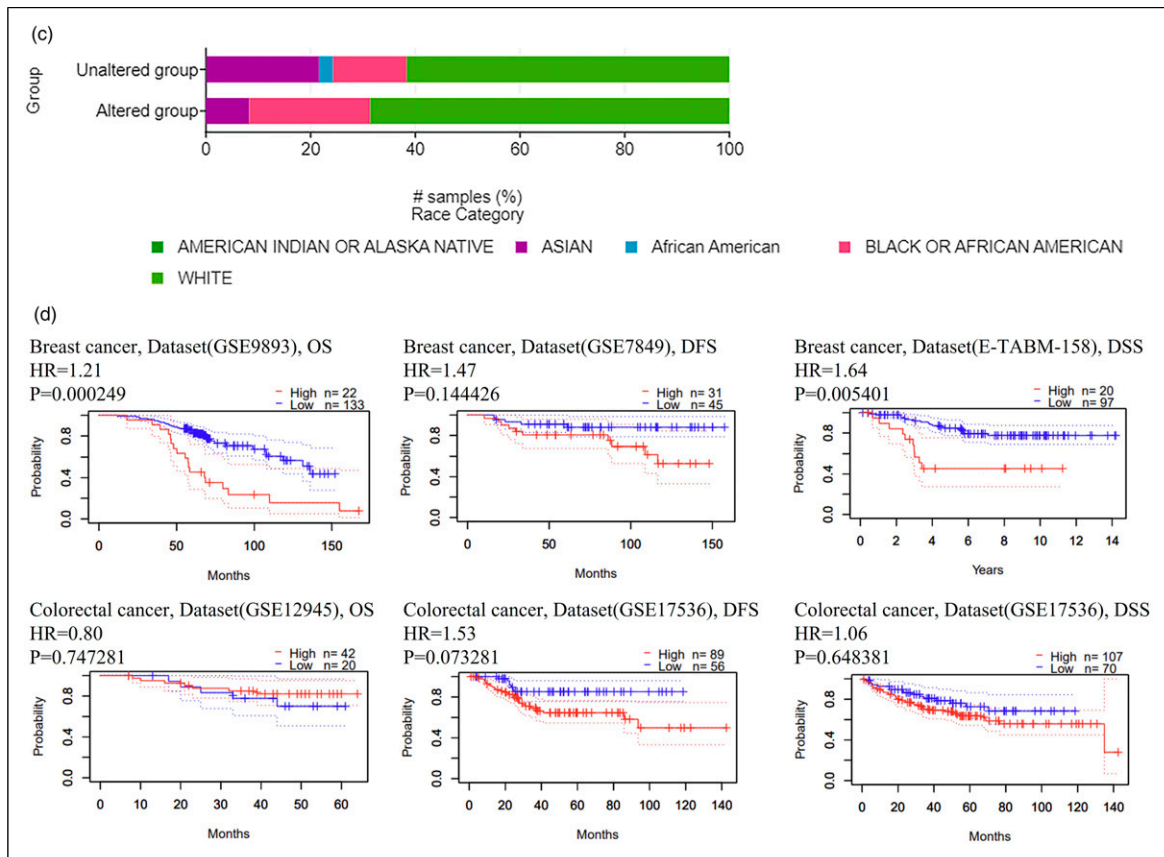


Figure 1. Continued.

pcDNA-MUC1 and PLXIN-MUC1 vectors by restriction enzyme mapping and sequencing (data not shown). Their schematic diagrams are illustrated in Figure 2. MUC1 was expressed on the cell surface of 293 cells after transient transfection with pcDNA-MUC1 and either the CT26 or TA3HA clone with transduced PLXIN-MUC1 (Figure 3(a)). To examine the expression pattern, we used an anti-endothelial antibody against the protein backbone. Flow cytometry results showed that MUC-1 was expressed as a glycosylated protein on all cell surfaces. We also performed immunoblotting to characterize MUC1 and compare it with the naturally expressed form using antibodies similar to that used in flow cytometry. We used protein extracts from MCF7 human breast cancer cells (lane 5) and MUC1 fusion protein comprising 5-VNTR repeats (lane 6) as positive controls. As presented in Figure 3(b), MUC1 expressed by pcDNA-MUC1 or by PLXIN-MUC1 was a single band of approximately 200 kDa, indicating a homogeneous glycosylation pattern. They comprised VNTR and non-VNTR, which were similar to naturally expressed human MUC1 on MCF7. The extracts from 293-pcDNA3.1 and CT26-PLXIN served as negative controls (lanes 1 and 3), with no bands being shown.

In vivo MUC1 location and expression

Female 6-week-old BALB/c mice were intradermally injected with 200 μ g, 100 μ g in each thigh, of pcDNA-MUC1 or pcDNA3.1. At the designated times, immunized mice were sacrificed, and the total DNA was extracted from the skin, including the injection site, and used for PCR to locate MUC1 DNA. MUC1 DNA was detected over 2 weeks post-vaccination (Figure 4(a)). We also evaluated MUC1 gene expression using RT-PCR, and the total RNA extracted from the injection site was used as a template. MUC1 RNA was also detected over 2 weeks post-vaccination (Figure 4(b)). These results suggest that injected DNA is present and expressed over 2 weeks after being transfected *in vivo*.

Immune cell repertoire

Immune cells were prepared in the spleen, mesenteric LNs, non-draining LNs, and draining LNs from immunized mice. The immune cells were stained with CD3 for T cells, CD22 for B cells, CD8 or CD4 for CD3 subsets, or CD40 for activated T cells, especially CD4 T cells. CD3-positive T cells were dominant in MUC-1-immunized draining LN cells, especially CD8-positive cytotoxic T cells (Figure

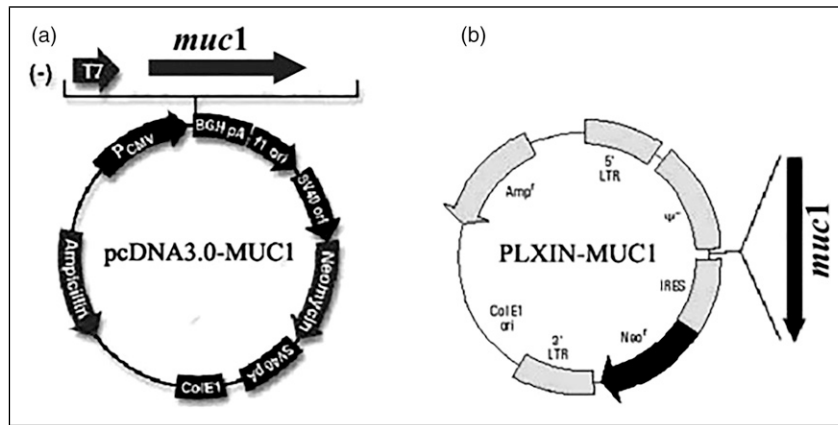


Figure 2. Schematic diagram for *MUC1* constructs. (a) pcDNA3.0-*MUC1* (pcDNA-*MUC1*). Human *MUC1* was sub-cloned from the APR-*MUC1* cloning vector into the pcDNA3.0 expression vector (Invitrogen), which was controlled using a CMV promoter, which also contains a neomycin resistance gene under the control of a SV40 promoter. (b) PLXIN-*MUC1*. Human *MUC1* was sub-cloned from the APR-*MUC1* cloning vector into the PLXIN retroviral vector (Invitrogen), which was controlled using a 5' LTR promoter, which also contains a neomycin resistance gene under the control of an IRES promoter.

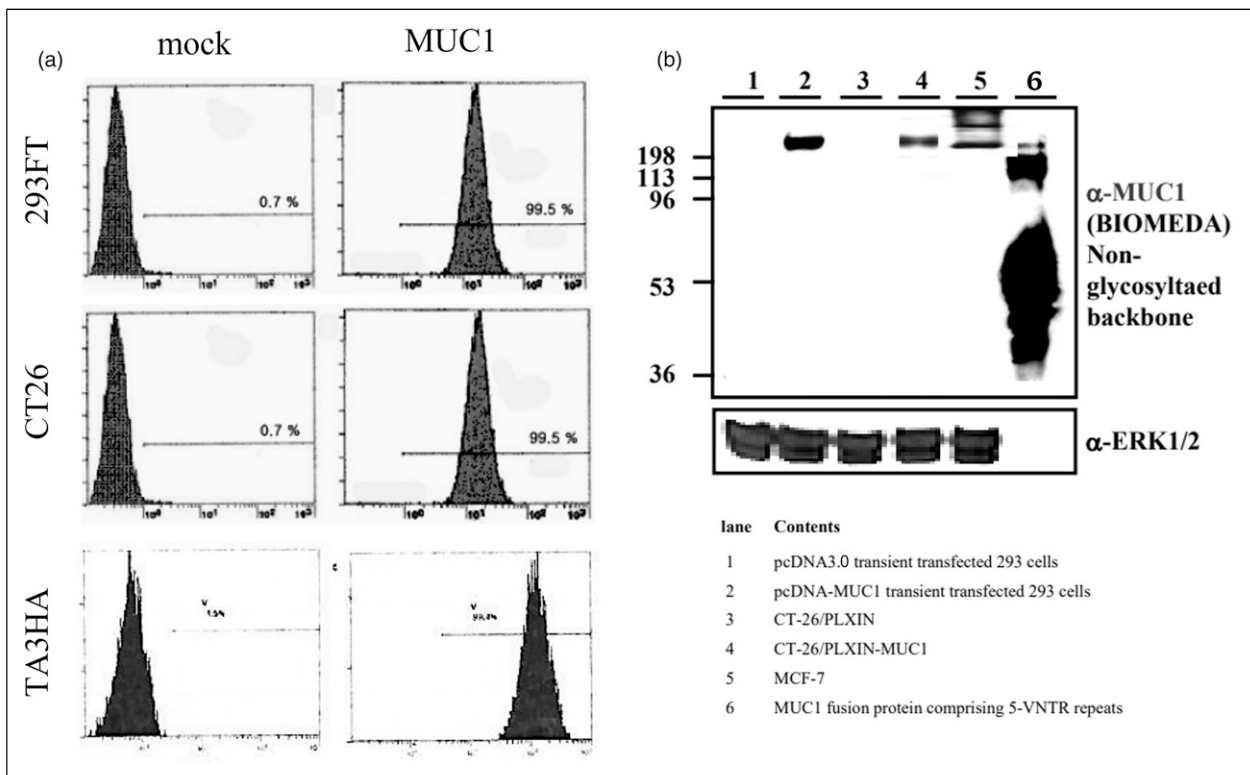


Figure 3. *In vitro* expression of *MUC1*. (a) Flow cytometric analysis of *MUC1* cell surface expression on 293 *MUC1*-transiently transfected cells and *MUC1*-transduced CT26 or TA3HA cell lines. (b) Western blotting. Protein was extracted from 293 *MUC1*-transiently transfected cells and *MUC1*-transduced CT26 cell lines; they were immunoblotted for the presence of *MUC1*. Lysates from MCF7 cell lines (lane 5) and mock vector-transfected, or -transduced cells (lanes 1 and 3) served as the positive and negative controls, respectively.

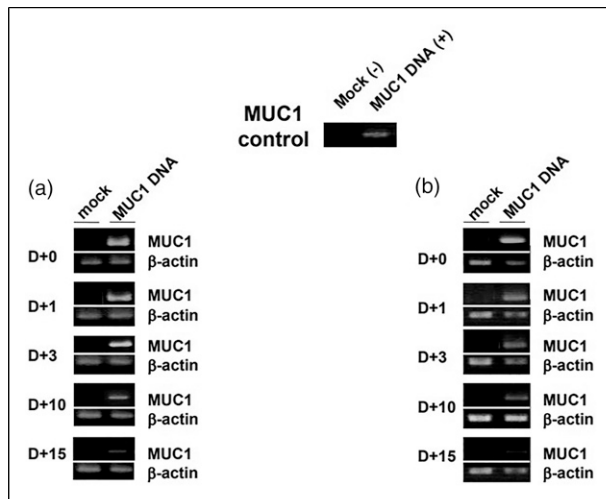


Figure 4. *In vivo* expression of *MUC1* DNA. DNA immunized lingual skin was prepared and DNA or RNA was extracted. *MUC-1* existence was monitored in DNA PCR (a), and the gene expression was monitored in RT-PCR (b).

5(a)). Draining LN cells were restimulated with PMA/ionomycin to detect T cell activation (Figure 5(b)). The CD3 portion was high in MUC-1-immunized mice draining LN cells, and CD40⁺CD4 T cells were high in MUC-1-immunized mice draining LN cells, suggesting that MUC-1 immunization induces Th1-dependent immunity.

These effects were also monitored in tumor-bearing mice draining LNs 30 days after tumor inoculation (Figure 6). In the MUC-1-immunized group, CD3-positive T cells were dominant, especially CD8 T cells. However, Mac1 was high in the pcDNA-immunized group, implying the presence of suppressive monocytes.

This result confirms that MUC-1 immunization induces T cell-dependent immunity, especially CD8 cytotoxic T cells.

Immune responses to *MUC1*

To determine MUC1-specific T cell response, we used intracellular FACS and ELISpot assay. Two weeks post-vaccination, the spleen, non-draining LNs, and draining LNs were extracted from the immunized mice, and lymphocytes were restimulated *in vitro* for 48 h with CT26 or CT26-MUC1. INF- γ -positive cells were detected in the spleen immunized with MUC1 DNA, but IL-4-positive cells were detected in the spleen immunized with pcDNA (Figure 7(a)). Moreover, draining LN cells were stimulated with PMA/ionomycin, and INF- γ -positive CD8 T cells were detected in the MUC1 DNA-immunized group (Figure 7(b)). In the ELISpot assay, an image of the spots was captured; subsequently, the intensity of spots in each

well was counted (Figure 8(a)). As a result, CD8⁺ INF- γ spots were high in the spleen and LN cells from NIS-immunized mice, but there was no difference in IL-4 levels.

In addition, mice were eye-bled 1-week post-immunization, and serum samples drawn were assayed for anti-MUC1 antibodies using ELISA plates coated with a synthetic peptide corresponding to the MUC1 tandem repeats (Figure 8(b)). The levels of anti-MUC1 antibody were higher compared with those of the sera from pcDNA3.0-immunized mice, which did not show any reactivity.

Taken together, immunization with pcDNA-MUC1 induced either MUC1-specific Th1 immune response or humoral response (high INF- γ secreting T cells and high Igs).

Tumor growth

BALB/c mice were intradermally immunized three times at 2-weeks intervals with plasmid DNA, pcDNA-MUC1, or pcDNA3.1. Immunized mice were challenged with MUC1 expressing tumor cells to examine an induction of immune response following DNA vaccination. Moreover, 5×10^4 or 5×10^5 CT26-MUC1 cells or 1×10^5 TA3HA-MUC1 cells were inoculated into mice 2 weeks post-final vaccination. We examined tumor growth; it was calculated twice a week after tumor inoculation (Figure 9(a) [CT26-MUC1 cells], Figure 9(b) [TA3HA-MUC1 cells]). All mice in the pcDNA3.0 DNA-immunized group developed large intra-abdominal masses of tumor but not those in the pcDNA-MUC1-immunized mice group. The rate of tumor growth in pcDNA-MUC1-immunized mice was also significantly lower than that observed in the control mice ($p < 0.001$).

These results suggest that in the control vaccines, pcDNA3.0 exhibited no inhibitory effect on the growth of the primary tumor. However, pcDNA-MUC1 DNA vaccination inhibited the rate of tumor growth.

Discussion

In this study, we provided evidence for the immunopotency, especially tumor infiltration capacity, of a MUC1 DNA vaccine against cancer.

Despite various attempts to kill cancer targeting MUC1 antigens, most were not effective. In this study, we focused on the following points: (1) peptide or protein MUC1 vaccines resulted in ineffective humoral immunity, although they were modulated to be more immunogenic,^{11–13} and (2) heterogeneous glycosylation patterns induced relatively low potency of tumor immunity as they stimulated multiple T cell epitopes at once.¹⁸ To solve these, the vaccine, pcDNA-MUC1, was designed to upregulate immune potency using a natural form of MUC1 (a) expressing a whole protein containing 42 tandem repeats and

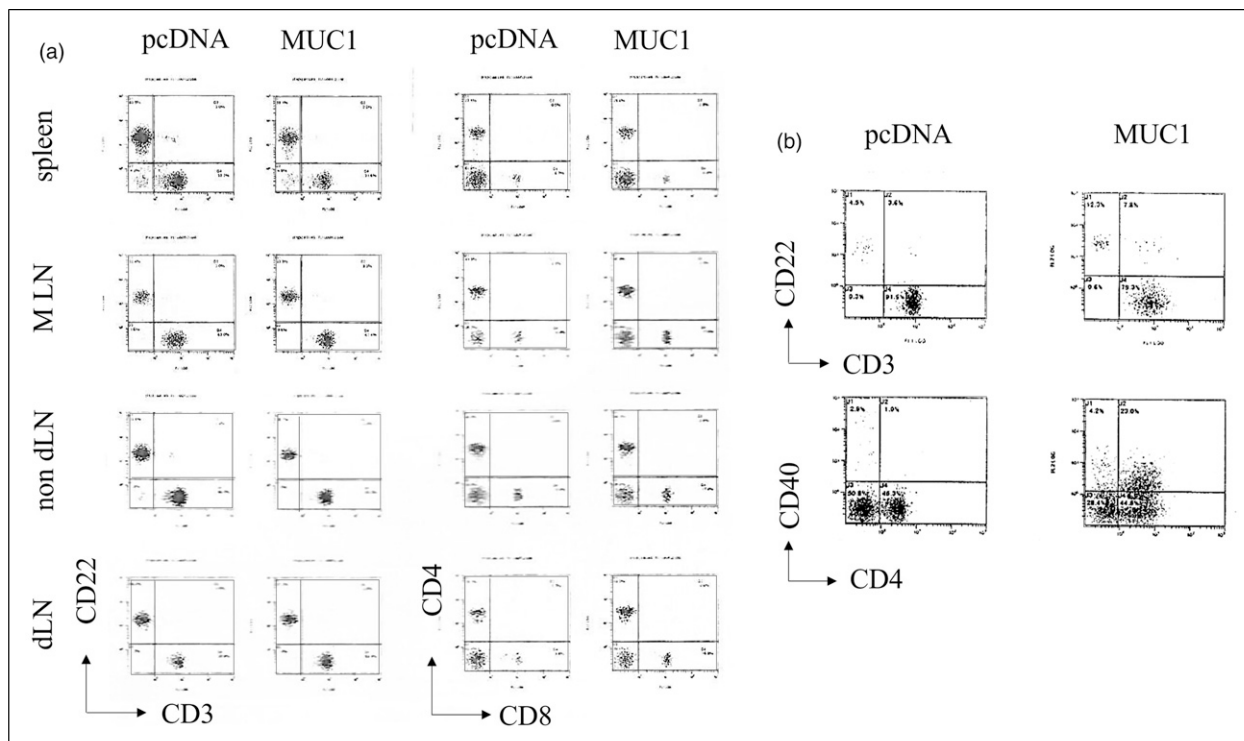


Figure 5. Immune cell population after triple immunization. One week after final immunization, spleen, draining LN, non-draining LN, and mesenteric LN cells were prepared. (a) T and B cell population, and CD4 and CD8 portions were determined, (b) PMA/ionomycin stimulated draining LN cells were discriminated from CD40 positive CD4 T cells.

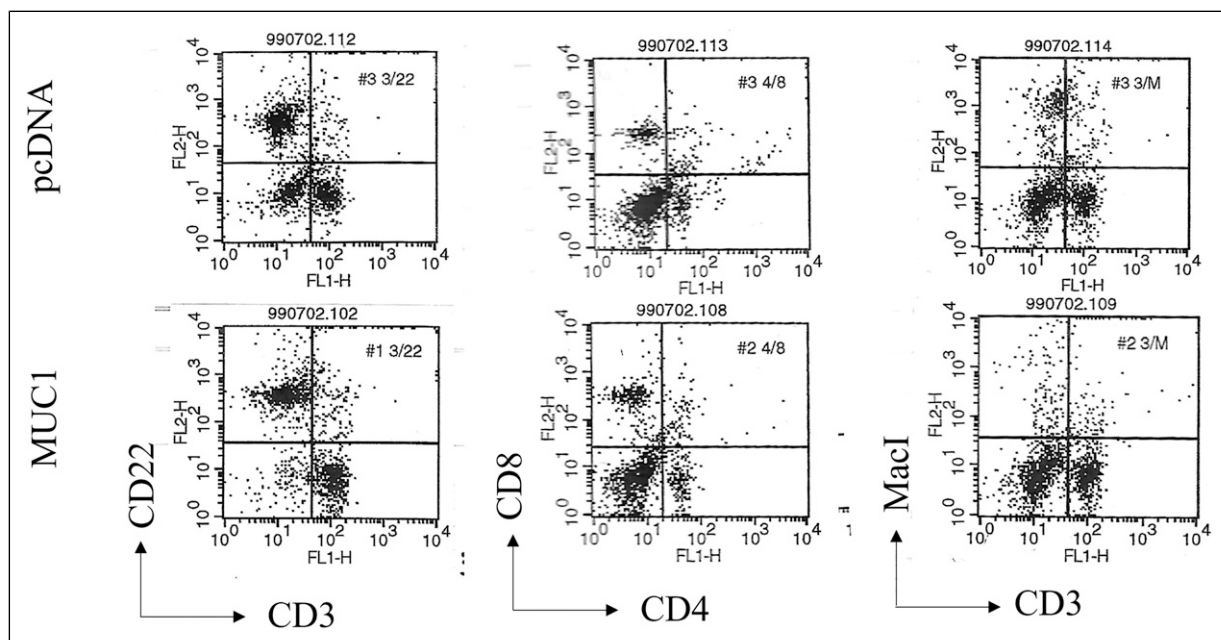


Figure 6. Immune cell population after tumor inoculation. Thirty days after tumor inoculation in MUC1 immunized mice, draining LN cells were prepared and subpopulations were monitored. CD3 for T cells; CD22 for B cells; CD4 or CD8 for T cells; and CD3⁺Mac1⁺ cells for immunosuppressive cells.

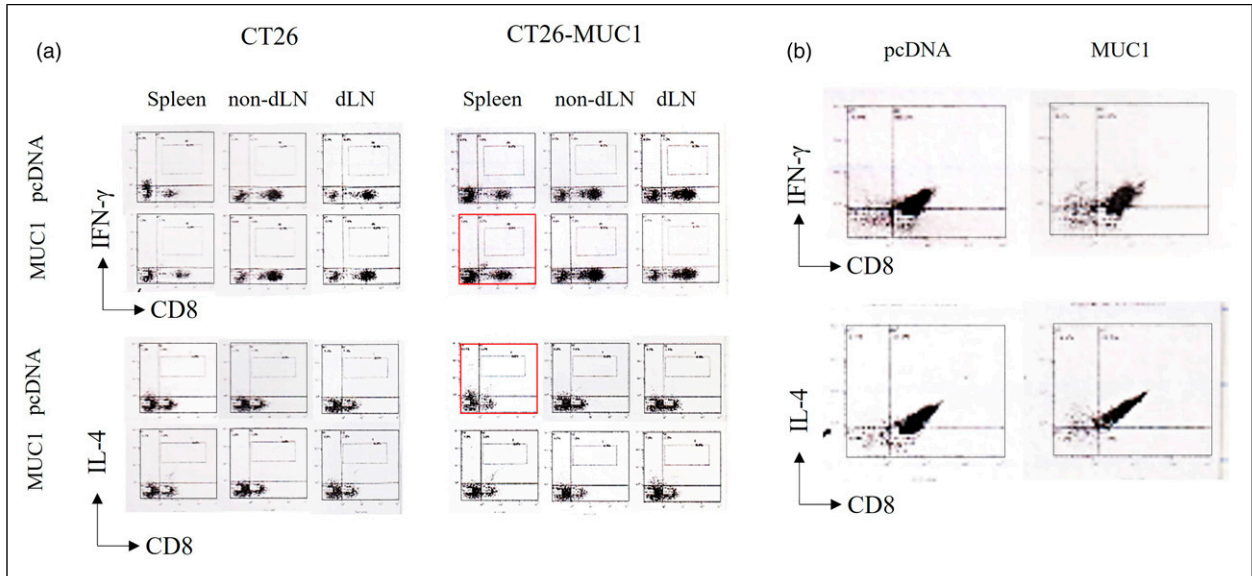


Figure 7. Immune cell activation. Intracellular FACS (IFN-g or IL-4) in spleen, draining LN, or non-draining LN cells prepared 1 week after final immunization. (a) pcDNA or *MUC1* DNA restimulation and (b) PMA/ionomycin restimulation.

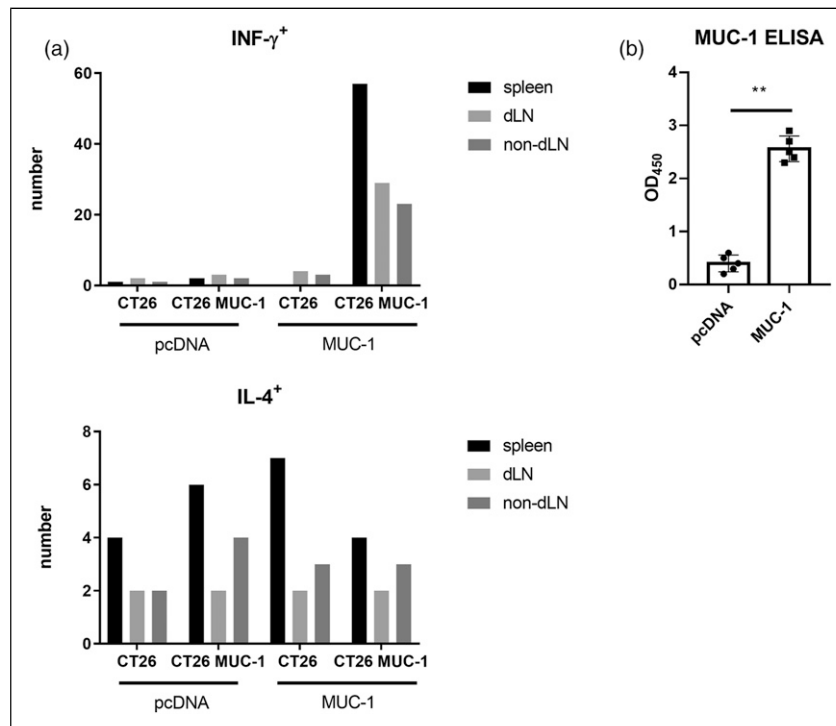


Figure 8. MUC-I specific immunity. MUC-I specific immunity was monitored 1 week after triple immunization. (a) ELISPOT (IFN-g or IL-4) in spleen, draining LN, or non-draining LN cells and (b) MUC-I specific humoral immunity.

N- and C-termini, derived from a pancreatic tumor; (b) expressing an underglycosylated protein; and (c) stimulating an effective adaptive immune response *in vivo* to kill cancer.

It has previously been shown that the lower-molecular-weight range refers to the early intermediate non-glycosylated form of mucin produced during

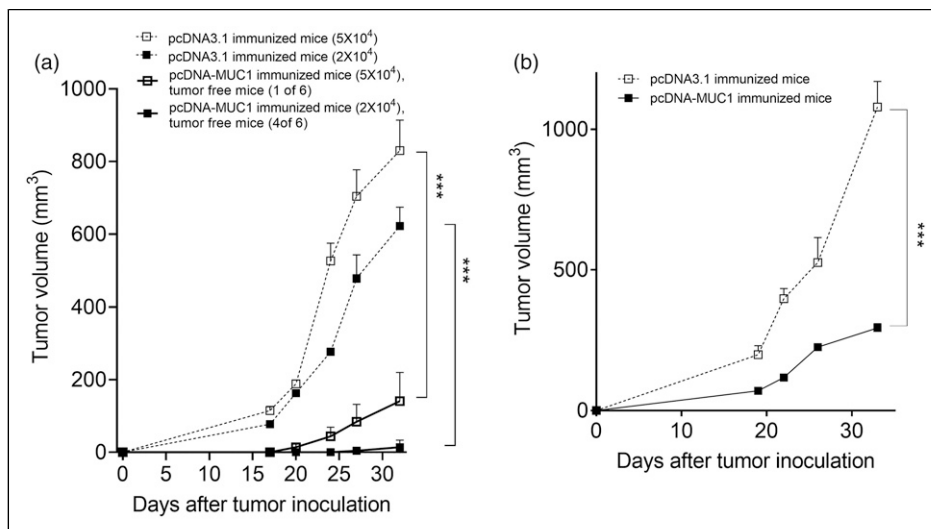


Figure 9. Tumor growth. Mean tumor volume after tumor engraftment in animals immunized with pcDNA-MUC1 or pcDNA3.0. Mice were inoculated with (a) 5×10^4 or 5×10^5 CT26-MUC1 tumor cells or (b) 5×10^5 TA3HA-MUC1 tumor cells, 2 weeks post-final immunization. We used more than 6 mice per group.

biosynthesis, and the lower band refers to the protein after cleavage of a 20-amino acid signal peptide.¹⁸ The fully glycosylated protein of 22 tandem repeats showed an apparent mass of >200 kDa,⁴⁹ and the underglycosylated form appeared in malignant cancers.⁸ As seen in Figure 3, the expression of MUC1 was likely to be an underglycosylated malignant form; it was a single peptide of approximately 400 kDa, advantageous for its use as a cancer vaccine. In addition, mRNA corresponding to *MUC1* was detected in mice immunized with *MUC1* DNA (Figure 4).

In the analysis of the ability of the *MUC1* plasmid vector to inhibit the growth of xenografted *MUC1* transducing cancer cells, tumors in pcDNA-MUC1-immunized mice grew significantly more slowly than the tumors observed in animals immunized with the control vector (Figure 9). Our observations indicate that three intradermal injections of *MUC1* cDNA suppress the development of *MUC1* expressing cancer cells in BALB/c mice and this occurs in an *MUC1*-specific manner. These results are significant, as *MUC1* is a major carcinoma-associated antigen that is known to induce immune responses in many patients with epithelial cancer.

DNA vaccination by intradermal injection has widely been shown to elicit immune responses against translated polypeptides.^{50–52} In line with this, we found that *MUC1* DNA vaccination results in the production of antibodies that are reactive with a synthetic *MUC1* peptide, a highly glycosylated *MUC1* protein purified from human milk, and CT26-MUC1 cells (Figure 8(b); data not shown). It was evident from our results that humoral immune responses specific for *MUC1* were induced. It is

hypothesized that when plasmid DNA is intradermally injected, keratinocytes or dermal DCs transcribe the DNA.^{53–56} The antibodies generated by *MUC1* DNA vaccination imply that antibody class switching had occurred, indicating that the *MUC1* DNA vaccine also primes $CD4^+$ T cells, which mediate such class switches. To confirm this, we also confirmed the cytokine repertoire through intracellular FACS (Figure 7) using lymphocytes from the spleen, draining LNs, non-draining LNs, and ELISpot (Figure 8(a)) from draining LNs after *MUC1* DNA vaccination. Intradermal injection of *MUC1* DNA initiated predominantly $IFN-\gamma$ -producing T cells. To assess whether this Th1-type dominant phenomenon is also effective in tumor regression, splenocytes were prepared at 1-month post-tumor inoculation and used for FACS. At that time, when $CD8^+$ T cells were dominant, immunosuppressive Mac1 cells were not in the *MUC1*-immunized group.

A single transfer of restimulated bone marrow cells from patients with breast cancer caused regression of xenografted autologous tumors in NOD/SCID mice.⁵⁷ Such a phenomenon has also been observed in *MUC1* transgenic mice, in which *MUC1* specific T cells were effective in controlling mammary gland and melanoma tumors. However, human cancer cells have their own low-level humoral and cellular immune reactions to several antigens including *MUC1*.⁵⁸ As this kind of native response makes it difficult to eradicate tumors through DNA vaccines, further experiments devising strategies to obtain effective immune responses are needed.

In conclusion, we constructed a novel *MUC1* DNA vaccine expressing a whole protein with 42 tandem

repeats for cancer prevention. Our vaccine, pcDNA-MUC1, inhibited the growth of MUC1 expressing cancer in BALB/c mice, which was in line with Th1 immune response. Moreover, CD8-positive T cell infiltration is important in killing tumors. Future experiments are planned to engineer vaccines to improve the efficacy of tumor immunity.

Conclusion

In this study, the immunopotency of the tumor infiltration capacity of a MUC1 DNA vaccine against cancers has been shown. After constructing a MUC1 DNA vaccine expressing a whole protein of 42 tandem repeats, injecting pcDNA-MUC1 inhibited the growth of MUC1 expressing cancer in BALB/c mice, which was in line with Th1 immune response. Further study regarding CD8-positive T cell infiltration will enhance the effectiveness of the vaccine against cancer.

Acknowledgements

The authors thank Dr Ji-Gwang Jung for advice on experimental design and statistical analysis.

Author contributions

H-YS contributed to the conception and design of the study. H-YS and H-KJ wrote sections of the manuscript. All authors contributed to the manuscript revision and read and approved the submitted version.

Declaration of conflicting interests

The author(s) declared no potential conflicts of interest with respect to the research, authorship, and/or publication of this article.

Funding

The author(s) disclosed receipt of the following financial support for the research, authorship, and/or publication of this article: This work was supported by the grant no. 04-2021-0570 from SNUH Research Fund.

Ethics approval

Ethical approval for this study was obtained from Institutional Review Board (IRB) of Seoul National University Hospital (H-1707-174-874).

Animal welfare

The present study followed international, national, and/or institutional guidelines for humane animal treatment and complied with relevant legislation.

ORCID iDs

Hye-Youn Son  <https://orcid.org/0000-0003-4929-0849>

Hwan-Kyu Jeong  <https://orcid.org/0000-0001-5652-3239>

Vasso Apostolopoulos  <https://orcid.org/0000-0001-6788-2771>

References

1. Siddiqui J, Abe M, Hayes E, YuMUC1 E and Kufe D (1987) Isolation and sequencing of a cDNA coding for the human DF3 breast carcinoma-associated antigen. *Proc Natl Acad Sci USA* 85: 2320–2323.
2. Croce MV, Colussi AG, Price MR and Segal-Eiras A (1997) Expression of tumour associated antigens in normal, benign and malignant human mammary epithelial tissue: a comparative immunohistochemical study. *Anticancer Res* 17: 4287–4292.
3. Irimura T, Denda K, Iida S, Takeuchi H and Kato K (1999) Diverse glycosylation of MUC1 and MUC1: potential significance in tumor immunity. *J Biochem* 126: 975–985.
4. Burchell J and Taylor-Papadimitriou J (1993) Effect of modification of carbohydrate side chains on the reactivity of antibodies with core-protein epitopes of the MUC1 gene product. *Epithelial Cell Biol* 4: 155–162.
5. Girling A, Bartkova J, Burchell J, Gillett C and Taylor-Papadimitriou J (1989) A core protein epitope of the polymorphic epithelial mucin detected by the monoclonal antibody SM-3 is selectively exposed in a range of primary carcinomas. *Int J Cancer* 43: 1072–1076.
6. Kotera Y, Fontenot D, Pecher G, Metzgar RS and Finn OJ (1994) Humoral immunity against a tandem repeat epitope of human mucin MUC1 in sera from breast, pancreatic, and colon cancer patients. *Cancer Res* 54: 2856–2860.
7. Bafna S, Kaur S and Kumar Batra S (2010) Membrane-bound mucins: the mechanistic basis for alterations in the growth and survival of cancer cells. *Oncogene* 29(20): 2893–2904.
8. Varki A, Kannagi R and Toole BP (2009) *Glycosylation Changes in Cancer, Essentials of Glycobiology*. 2nd edition. Cold Spring Harbor (NY): Cold Spring Harbor Laboratory Press.
9. Gilewski T, Adluri S, Ragupathi G, Zhang S, Yao TJ, Panageas K, et al. (2000) Vaccination of high-risk breast cancer patients with mucin-1 (MUC1) keyhole limpet hemocyanin conjugate plus QS-21. *Clin Cancer Res* 6: 1693–1701.
10. Soares MM, Mehta V and Finn OJ (2001) Three different vaccines based on the 140-amino acid MUC1 peptide with seven tandemly repeated tumor-specific epitopes elicit distinct immune effector mechanisms in wild-type versus MUC1-transgenic mice with different potential for tumor rejection. *J Immunol* 166: 6555–6563.
11. Karanikas V, Hwang L, Pearson J, Ong CS, Apostolopoulos V, Vaughan H, et al. (1997) Antibody and T cell responses of

- patients with adenocarcinoma immunized with mannan-MUC1 fusion protein. *J Clin Invest* 100: 2783–2792.
12. Apostolopoulos V, Osinski C and McKenzie IFC (1998) MUC1 cross reactive Gal α (1, 3)Gal Abs in humans switch immune responses from cellular to humoral. *Nat Med* 4: 315–320.
 13. Apostolopoulos V, Sandrin MS and McKenzie IFC (1999) Carbohydrate/peptide mimics: effect on MUC1 cancer immunotherapy. *J Mol Med* 77: 427–436.
 14. Gurunathan S, Klinman DM and Seder RA (2000) DNA vaccines: immunology, application, and optimization. *Annu Rev Immunol* 18: 927–974.
 15. Donnelly JJ, Ulmer JB and Liu MA (1997) DNA vaccine. *Life Sci* 60: 163–172.
 16. Maecker HT, Uematsu DT, DeKruyff RH, et al. (1998) Cytotoxic T cell responses to DNA vaccination: dependence on antigen presentation via class II MHC. *J Immunol* 161: 6532–6536.
 17. Henderson RA, Konitsky WM, Barrat-Boyes SM, Soares M, Robbins PD and Finn OJ (1998) Retroviral expression of MUC-1 tumor antigen with intact repeat structure and capacity to elicit immunity *in vivo*. *J Immunother* 21: 247–256.
 18. Stover CK, de la Cruz VF, Fuerst TR, Burlein JE, Benson LA, Bennett LT, et al. (1991) New use of BCG for recombinant vaccines. *Nature* 351: 456–460.
 19. Cerami E, Gao J, Dogrusoz U, Gross BE, Sumer SO, Aksoy BA, et al. (2012) The cBio cancer genomics portal: an open platform for exploring multidimensional cancer genomics data. *Cancer Discov* 2(5): 401–404. DOI: [10.1158/2159-8290.CD-12-0095](https://doi.org/10.1158/2159-8290.CD-12-0095) Erratum in: *Cancer Discov*. 2012 Oct;2(10):960. PMID: 22588877; PMCID: PMC3956037.
 20. Gao J, Aksoy BA, Dogrusoz U, Dresdner G, Gross B, Sumer SO, et al. (2013) Integrative analysis of complex cancer genomics and clinical profiles using the cBioPortal. *Sci Signal* 6(269): p11. DOI: [10.1126/scisignal.2004088](https://doi.org/10.1126/scisignal.2004088)
 21. Razavi P, Chang MT, Xu G, Bandlamudi C, Ross DS, Vasan N, et al. (2018) The genomic landscape of endocrine-resistant advanced breast cancers. *Cancer Cell* 34(3): 427–438.e6. DOI: [10.1016/j.ccell.2018.08.008](https://doi.org/10.1016/j.ccell.2018.08.008)
 22. Razavi P, Dickler MN, Shah PD, Toy W, Brown DN, Won HH, et al. (2020) Alterations in PTEN and ESR1 promote clinical resistance to alpelisib plus aromatase inhibitors. *Nat Cancer* 1(4): 382–393. DOI: [10.1038/s43018-020-0047-1](https://doi.org/10.1038/s43018-020-0047-1)
 23. Eirew P, Steif A, Khattra J, Ha G, Yap D, Farahani H, et al. (2015) Dynamics of genomic clones in breast cancer patient xenografts at single-cell resolution. *Nature* 518(7539): 422–426. DOI: [10.1038/nature13952](https://doi.org/10.1038/nature13952)
 24. Banerji S, Cibulskis K, Rangel-Escareno C, Brown KK, Carter SL, Frederick AM, et al. (2012) Sequence analysis of mutations and translocations across breast cancer subtypes. *Nature* 486(7403): 405–409. DOI: [10.1038/nature11154](https://doi.org/10.1038/nature11154)
 25. Smith AE, Ferraro E, Safonov A, et al. (2021) HER2+ breast cancers evade anti-HER2 therapy via a switch in driver pathway. *Nat Commun* 12(1): 1–10.
 26. Kan Z, Ding Y, Kim J, Jung HH, Chung W, Lal S, et al. (2018) Multi-omics profiling of younger Asian breast cancers reveals distinctive molecular signatures. *Nat Commun* 9(1): 1725. DOI: [10.1038/s41467-018-04129-4](https://doi.org/10.1038/s41467-018-04129-4)
 27. Pareja F, Brown DN, Lee JY, Da Cruz Paula A, Selenica P, Bi R, et al. (2020) Whole-exome sequencing analysis of the progression from non-low-grade ductal carcinoma in situ to invasive ductal carcinoma. *Clin Cancer Res* 26(14): 3682–3693. DOI: [10.1158/1078-0432.CCR-19-2563](https://doi.org/10.1158/1078-0432.CCR-19-2563)
 28. Nixon MJ, Formisano L, Mayer IA, Estrada MV, González-Ericsson PI, Isakoff SJ, et al. (2019) PIK3CA and MAP3K1 alterations imply luminal A status and are associated with clinical benefit from pan-PI3K inhibitor buparlisib and letrozole in ER+ metastatic breast cancer. *NPJ Breast Canc* 5: 31. DOI: [10.1038/s41523-019-0126-6](https://doi.org/10.1038/s41523-019-0126-6)
 29. Shah SP, Roth A, Goya R, Oloumi A, Ha G, Zhao Y, et al. (2012) The clonal and mutational evolution spectrum of primary triple-negative breast cancers. *Nature* 486(7403): 395–399. DOI: [10.1038/nature10933](https://doi.org/10.1038/nature10933)
 30. Rueda OM, Sammut SJ, Seoane JA, Chin SF, Caswell-Jin JL, Callari M, et al. (2019) Dynamics of breast-cancer relapse reveal late-recurring ER-positive genomic subgroups. *Nature* 567(7748): 399–404. DOI: [10.1038/s41586-019-1007-8](https://doi.org/10.1038/s41586-019-1007-8)
 31. Pereira B, Chin SF, Rueda OM, Vollan HK, Provenzano E, Bardwell HA, et al. (2016) The somatic mutation profiles of 2,433 breast cancers refines their genomic and transcriptomic landscapes. *Nat Commun* 7: 11479. DOI: [10.1038/ncomms11479](https://doi.org/10.1038/ncomms11479)
 32. Curtis C, Shah SP, Chin SF, Turashvili G, Rueda OM, Dunning MJ, et al. (2012) The genomic and transcriptomic architecture of 2,000 breast tumours reveals novel subgroups. *Nature* 486(7403): 346–352. DOI: [10.1038/nature10983](https://doi.org/10.1038/nature10983)
 33. Stephens PJ, Tarpey PS, Davies H, Van Loo P, Greenman C, Wedge DC, et al. (2012) The landscape of cancer genes and mutational processes in breast cancer. *Nature* 486(7403): 400–404. DOI: [10.1038/nature11017](https://doi.org/10.1038/nature11017)
 34. Guda K, Veigl ML, Varadan V, Nosrati A, Ravi L, Lutterbaugh J, et al. (2015) Novel recurrently mutated genes in African American colon cancers. *Proc Natl Acad Sci USA* 112(4): 1149–1154. DOI: [10.1073/pnas.1417064112](https://doi.org/10.1073/pnas.1417064112)
 35. Vasaikar S, Huang C, Wang X, Petyuk VA, Savage SR, Wen B, et al. (2019) Clinical proteomic tumor analysis consortium. Proteogenomic analysis of human colon cancer reveals new therapeutic opportunities. *Cell* 177(4): 1035–1049.e19. DOI: [10.1016/j.cell.2019.03.030](https://doi.org/10.1016/j.cell.2019.03.030)
 36. Giannakis M, Mu XJ, Shukla SA, Qian ZR, Cohen O, Nishihara R, et al. (2016) Genomic correlates of immune-cell infiltrates in colorectal carcinoma. *Cell Rep* 15(4): 857–865. DOI: [10.1016/j.celrep.2016.03.075](https://doi.org/10.1016/j.celrep.2016.03.075). Epub 2016 Apr 14 Erratum in: *Cell Rep*. 2016;17 (4):1206.

37. Seshagiri S, Stawiski EW, Durinck S, Modrusan Z, Storm EE, Conboy CB, et al. (2012) Recurrent R-spondin fusions in colon cancer. *Nature* 488(7413): 660–664. DOI: [10.1038/nature11282](https://doi.org/10.1038/nature11282).
38. Brannon AR, Vakiani E, Sylvester BE, Scott SN, McDermott G, Shah RH, et al. (2014) Comparative sequencing analysis reveals high genomic concordance between matched primary and metastatic colorectal cancer lesions. *Genome Biol* 15(8): 454. DOI: [10.1186/s13059-014-0454-7](https://doi.org/10.1186/s13059-014-0454-7)
39. Mondaca S, Walch H, Nandakumar S, Chatila WK, Schultz N and Yaeger R (2020) Specific mutations in APC, but not alterations in DNA damage response, associate with outcomes of patients with metastatic colorectal cancer. *Gastroenterology* 159(5): 1975–1978.e4. Epub 2020 Jul 27. PMID: 32730818; PMCID: PMC7680360. DOI: [10.1053/j.gastro.2020.07.041](https://doi.org/10.1053/j.gastro.2020.07.041)
40. Yaeger R, Chatila WK, Lipsyc MD, Hechtman JF, Cercek A, Sanchez-Vega F, et al. (2018) Clinical sequencing defines the genomic landscape of metastatic colorectal cancer. *Cancer Cell* 33(1): 125–136.e3. DOI: [10.1016/j.ccell.2017.12.004](https://doi.org/10.1016/j.ccell.2017.12.004)
41. Ganesh K, Wu C, O'Rourke KP, et al. (2019) A rectal cancer organoid platform to study individual responses to chemoradiation. *Nat Med* 25: 1607–1614. DOI: [10.1038/s41591-019-0584-2](https://doi.org/10.1038/s41591-019-0584-2)
42. Cancer Genome Atlas Network (2012) Comprehensive molecular characterization of human colon and rectal cancer. *Nature* 487(7407): 330–337. DOI: [10.1038/nature11252](https://doi.org/10.1038/nature11252)
43. *The Cancer Genome Atlas* <https://tcga-data.nci.nih.gov/tcga/>. Access date Jan 10, 2022.
44. Mizuno H, Kitada K, Nakai K and Sarai A (2009) PrognScan: a new database for meta-analysis of the prognostic value of genes. *BMC Med Genomics* 2: 18.
45. Zöller M and Christ O (2001) Prophylactic tumor vaccination: comparison of effector mechanisms initiated by protein versus DNA vaccination. *J Immunol* 166: 3440–3450.
46. Apostolopoulos V, Xing PX, Trapani JA and McKenzie IFC (1993) Production of anti-breast cancer monoclonal antibodies using a glutathione-S-transferase-MUC1 bacterial fusion protein. *Br J Cancer* 67: 713–720.
47. Dubey P, Su H, Adonai N, Du S, Rosato A, Braun J, et al. (2003) Quantitative imaging of the T cell antitumor response by positron-emission tomography. *Proc Natl Acad Sci U S A* 100: 1232–1237.
48. Oran AE and Robinson HL (2003) DNA vaccines, combining form of antigen and method of delivery to raise a spectrum of IFN- γ and IL-4-producing CD4+ and CD8+ T cells. *J Immunol* 171: 1999–2005.
49. Ciborowski P and Finn OJ (2000) Expression of MUC1 in insect cells using recombinant baculovirus. *Met Mol Biol* 125: 971–986.
50. Akbari O, Panjwani N, Garcia S, Tascon R, Lowrie D and Stockinger B (1999) DNA vaccination: transfection and activation of dendritic cells as key events for immunity. *J Exp Med* 189: 169–177.
51. Porgador A, Irvine KR, Iwasaki A, Barber BH, Restifo NP and Germain RN (1998) Predominant role for directly transfected dendritic cells in antigen presentation to CD8 T cells after gene gun immunization. *J Exp Med* 188: 1075–1082.
52. Ito K, Ito K, Shinohara N and Kato S (2003) DNA immunization via intramuscular and intradermal routes using a gene gun provides different magnitudes and durations on immune response. *Mol Immunol* 39: 847–854.
53. Song ES, Lee V, Surh CD, et al. (1997) Antigen presentation in retroviral vector-mediated gene transfer *in vivo*. *Proc Natl Acad Sci USA* 94: 1943–1948.
54. Condon C, Watkins SC, Celluzzi CM, et al. (1996) DNA-based immunization by *in vivo* transfection of dendritic cells. *Nat Med* 2: 1122–1128.
55. Iwasaki A, Torres CA, Ohashi PS, et al. (1997) The dominant role of bone marrow-derived cells in CTL induction following plasmid DNA immunization at different sites. *J Immunol* 159: 11–14.
56. La Cava A, Billetta R, Gaietta G, et al. (2000) Cell-mediated DNA transport between distant inflammatory sites following intradermal DNA immunization in the presence of adjuvant. *J Immunol* 164: 1340–1345.
57. Feuerer M, Beckhove P, Bai L, Solomayer EF, Bastert G, Diel IJ, et al. (2001) Therapy of human tumors in NOD/SCID mice with patient-derived reactivated memory T cells from bone marrow. *Nat Med* 7: 452–458.
58. Mukherjee P, Ginardi AR, Tinder TL, Sterner CJ and Gendler SJ (2001) MUC1-specific cytotoxic T lymphocytes eradicate tumors when adoptively transferred *in vivo*. *Clin Cancer Res* 7: 848s–855s.